

Sampling from Pre-Images to Learn Heuristic Functions for Classical Planning

Stefan O’Toole¹, Miquel Ramirez², Nir Lipovetzky¹, Adrian R. Pearce¹

¹ Computing and Information Systems, University of Melbourne, Australia

² Electrical and Electronic Engineering, University of Melbourne, Australia

stefan@student.unimelb.edu.au, {miquel.ramirez, nir.lipovetzky, adrianrp}@unimelb.edu.au

Abstract

We introduce a new algorithm, *Regression based Supervised Learning* (RSL), for learning per instance Neural Network (NN) defined heuristic functions for classical planning problems. RSL uses regression to select relevant sets of states at a range of different distances from the goal. RSL then formulates a Supervised Learning problem to obtain the parameters that define the NN heuristic, using the selected states labeled with exact or estimated distances to goal states. Our experimental study shows that RSL outperforms, in terms of coverage, previous classical planning NN heuristic functions while requiring two orders of magnitude less training time.

Introduction

Heuristics for automated planning can be formulated following a number of approaches. Heuristics such as Fast-Forward (FF) (Hoffmann and Nebel 2001), h^{\max} and h^{add} (Bonet, Loerincs, and Geffner 1997) follow from analyzing the structure of many planning instances, and coming up with a mathematical framework to automatically compute functions that capture important structural information about instances from the symbolic descriptions of causal laws (actions) and domain constraints (Helmert 2006). Alternatively, Pattern database (Edelkamp 2014) and *merge-and-shrink* (Helmert et al. 2007) heuristics are defined as generic functions that evaluate states by projecting them onto many smaller sub-problems, that are solved optimally, and combining their solutions in some specific way. These are chosen on a per-instance basis, and typically involve solving a discrete optimization problem to select which projection is deemed to be most informative according to some suitably defined criterion. A third approach has attracted attention recently, where heuristic functions are searched for in a family of functions described by a Neural Network (NN) (Ferber et al. 2021; Ferber, Helmert, and Hoffmann 2020; Shen, Trevizan, and Thiébaux 2020). These efforts are mainly driven by the suggestive results in Computer Vision and Reinforcement Learning of novel, general, and scalable stochastic algorithms for convex optimization to select NN parameters that minimize a suitably defined notion of *empirical risk* (Kingma and Ba 2015; Goodfellow, Bengio,

and Courville 2016; Hardt and Recht 2021). Currently, the most successful methods for learning NN heuristics for classical planning problems require vast amounts of computational resources for training and are usually outperformed by heuristics that do not require any offline training time (Ferber et al. 2021).

In this work, we introduce the *Regression based Supervised Learning* (RSL) algorithm in order to learn per instance NN defined heuristic functions. Like other methods (Ferber et al. 2021; Yu, Kuroiwa, and Fukunaga 2020) do, RSL selects a set of *regressions*, trajectories of *sets of states*, or *pre-images*, found via the application of well-known and efficient pre-imaging operators (Rintanen 2008) that rely on symbolic action descriptions. These trajectories found along a given regression, always start from the set of goal states of an instance, and then training states are sampled from each set along the trajectory. Our method takes many samples from each pre-image found in a regression, instead of performing many trajectories or longer regressions to increase the number of training states for the NN, using the observed goal distances for each pre-image to label the sampled states.

Through a sensitivity analysis over RSL’s hyper-parameters we explore the impact of its key mechanisms. We also benchmark the NN heuristics learnt by RSL against existing methods to provide insight into the ability of RSL to learn effective heuristics. The paper’s contributions are threefold: (1) introducing a new method for training NN defined heuristic functions, (2) introducing a new novelty measure for a regression based search, and (3) an experimental analysis of RSL’s hyper-parameters and components.

Background

Classical Planning. We consider classical planning problems as defined by the STRIPS formulation (Fikes and Nilsson 1971). STRIPS defines a planning problem as the tuple $\Pi = \langle F, O, I, G \rangle$, where F is a set of atoms, O is a set of actions, $I \subseteq F$ is the initial state and $G \subseteq F$ is the goal set. Each action $a \in O$ is represented by the tuple $\langle \text{Add}(a), \text{Del}(a), \text{Pre}(a) \rangle$ which are each a set of atoms over F . $\text{Add}(a)$ and $\text{Del}(a)$ describe the atoms that are added and removed from the state respectively, and $\text{Pre}(a)$ describes the atoms that must be true in a state in order to apply action a . The STRIPS problem Π implicitly represents

in a compact form a deterministic transition system (Geffner and Bonet 2013). The classical planning state-transition model for progression is $\mathcal{S}(\Pi) = \langle S, s_0, S_G, A, f, c \rangle$, where $S \subseteq 2^F$, s_0 is the initial state I , S_G is the set of goal states described as the set $\{s \mid s \supseteq G, s \in S\}$, the actions $a \in A(s)$ are the actions in O that are applicable in s , that is $Pre(a) \subseteq s$, f is the transition function where for action a and state s , the resulting state is $s' = f(a, s) = (s \setminus Del(a)) \cup Add(a)$, and finally $c(a, s)$ is the cost of selecting the transition out of s via action a . The problems we consider in this paper all have a uniform cost $c(a, s) = 1$. A solution for a classical planning problem is a sequence of actions a_0, \dots, a_n that select transitions connecting the initial state s_0 to a state within the goal set S_G . The progression state-transition model can be used to find a solution through a forward search for a goal state from s_0 .

Heuristics. The objective of the heuristics introduced in this paper is to approximate the optimal value function V^* as described through the Bellman optimality equation (Bellman 1957),

$$V^*(s) = \min_{a \in A(s)} \left[c(a, s) + V^*(f(a, s)) \right] \quad (1)$$

for all states $s \notin S_G$ and $V^*(s) = 0$ for $s \in S_G$. Similar to many of the existing heuristics such as h^{FF} the heuristics introduced in this paper are not guaranteed to be lower or upper bounds on the optimal value function.

Regression. Planners can also search backwards from the goal through the regression state-transition model (Geffner and Bonet 2013). The regression state-transition model is $R(\Pi) = \langle S, s_0, S_G, A, f, c \rangle$, where s_0 is the partially assigned state G , the goal set S_G is the set $\{s \mid s \subseteq I, s \in S\}$, $A(s)$ are the actions in O that are relevant and consistent for the partial state s , that is $Add(a) \cap s \neq \emptyset$ and $Del(a) \cap s = \emptyset$, and the state transition function to pre-image state s is $f(a, s) = (s \setminus Add(a)) \cup Pre(a)$. A key difference between the regression and progression state-transition models is that the regression model searches over partial truth assignments, which represent sets of states as opposed to complete truth-assignments. For the progression state-transition model every atom not in a state is false, while for the regression state-transition model the atoms not in a state are simply undefined. From this point forward we refer to such “partial states” as *pre-images* and denote them as x to distinguish them from complete truth-assignment state denoted as s . The regression model is required to search over pre-images $x \subseteq F$ as the initial pre-image x_0 coincides with the set of goal states from the progression state-transition model S_G . Regression operators also compute *weaker pre-conditions* so the only atoms being asserted in a pre-image x are those in the precondition $Pre(a)$, while retracting any commitments on the truth value of atoms in $Add(a)$. Conversely, the progression state model will always search over full states $s \in \mathcal{S}(\Pi)$ as I prescribes the truth value of every atom, and the progression transition function $f(a, s)$ provides an explicit mapping between states $s, s' \in \mathcal{S}(\Pi)$.

Supervised Learning. In this paper we take advantage of the pre-images explored by a regression search in order to sample a set of training states labelled with approximations

\tilde{V} of V^* (Equation 1), to learn a heuristic defined through a NN using a Supervised Learning (SL) algorithm.

SL is a common approach for creating predictors from data samples through empirical risk minimisation (Hardt and Recht 2021) with a goal of generalising to out-of-sample data. That is, the objective of SL given a function class $\mathcal{H} \subseteq \mathcal{X} \rightarrow \mathcal{Y}$ and a set of data samples $(\bar{x}_1, y_1), (\bar{x}_2, y_2), \dots, (\bar{x}_i, y_i)$ is defined as,

$$\min_{h \in \mathcal{H}} \frac{1}{n} \sum_{i=1}^n \text{loss}(h(\bar{x}_i), y_i) \quad (2)$$

In this paper, \mathcal{H} is a NN, each $h \in \mathcal{H}$ is a unique set of NN parameters θ , training examples \bar{x}_i are states s , and labels y_i are cost-to-go estimates \tilde{V} between s and S_G .

Per-instance heuristics. Ferber et al. (2021) describe two different methods for learning heuristics for classical planning problems. The first is *per domain* learning, where a heuristic is learnt that is applicable to any instance of a particular domain, where a domain defines a set of action schemas and predicates which are used to formulate instances Π . Our paper focuses on the second framework introduced by Ferber et al. (2021), which is to learn instance-based heuristics. That is, given some instance $\mathcal{S}(\Pi)$ with initial state s_0 , we seek heuristics h that apply to instances $\mathcal{S}(\Pi_1), \mathcal{S}(\Pi_2), \dots, \mathcal{S}(\Pi_i)$ where all the instances $\mathcal{S}(\Pi_i)$ share all structural elements with $\mathcal{S}(\Pi)$ but initial states. That is, each $\mathcal{S}(\Pi_i)$ features a distinct initial state s_0^i , which is reachable from s_0 in $\mathcal{S}(\Pi)$. Our objective in this work is to efficiently, in terms of computation time, create a data sample of states labelled with \tilde{V} such that an optimisation of the NN parameters θ using Equation 2 generalises to the population set of states s_0^i reachable from s_0 .

Related Work

Ferber et al. (2020) introduce a method, Teacher-based Supervised Learning (TSL), that constructs a training set out of states found in the trace of the execution of plans from a teacher planner. TSL performs 200 step random walks from the initial state of an instance and then uses a Greedy Best First Search (GBFS) with h^{FF} to search for a plan. The states along the solution path (if found) are labeled with an estimate of their distance from the goal according to the solution. TSL then performs Supervised Learning (SL) on the states and goal-distance estimates to learn a heuristic.

Yu et al. (Yu, Kuroiwa, and Fukunaga 2020) introduced an alternative SL method for learning per-instance heuristic functions. Yu et al.’s algorithm (SING) performs backwards depth-first searches (DFS) with fixed node expansion budgets, to search from fully assigned randomly sampled goal states $s_g \in S_G$. SING then uses SL on states visited within the DFS labeled with the depth at which the states were visited for an estimate of their goal distance.

The algorithm we introduce in this work differs from both TSL and SING in a number of ways. First, RSL samples training states through a regression over partially assigned states starting from the goal rather than a DFS starting at a fully assigned goal state (SING) or a forward search from the

instance’s initial state (TSL). Second, RSL additionally samples random states that are added to the training set. Third, for goal distance estimates TSL uses a teacher planner and SING uses the depth at which the state was visited while RSL uses the tightest upper bound found for the state’s goal distance derived through the pre-images visited by a number of regressions. Last, as RSL searches and labels goal distance estimates over pre-images, it samples many different training states from each pre-image.

More recently Ferber et al. (2021) introduced three new NN heuristics. Two of the approaches introduced, h^{Boot} and h^{BExp} , are based on the idea of training a heuristic on successively harder to solve states (Arfaee, Zilles, and Holte 2011). h^{Boot} and h^{BExp} , perform regressions from the goal following random walks, and solve using GBFS with the current h^{Boot} or h^{BExp} heuristic from a fully assigned state randomly sampled from the pre-image discovered by the regression. h^{Boot} uses the plan’s length while h^{BExp} uses the number of states expanded by GBFS as the state training labels for the estimated goal distance. h^{Boot} and h^{BExp} use the states and labels to iteratively train their NNs, and once the GBFS is solving 95% of the states found from the regressions, the maximum length of the regression is doubled. Ferber et al. (2021) also introduced the h^{AVI} heuristic which is trained using approximate value iteration. h^{AVI} , also discovers states through regressions but instead of solving for the state, h^{AVI} performs Bellman updates on a 2 step lookahead from the state, evaluating the leaf states of the lookahead with the current h^{AVI} heuristic or as 0 if they are goal states. Ferber et al.’s motivation for these Active Learning (AL) approaches verse SL ones is that SL is limited to instances small enough for training data generation.

Beyond learning per-instance NN defined heuristics, Shen et al.’s (2020) STRIPS Hypergraphs Networks (HGNs) learns per-domain and even domain independent NN defined heuristics. In this work we do not focus on domain independent NN defined heuristic functions, but we do compare against a STRIPS-HGN heuristic trained in a per-domain framework as described by Ferber et al. (2021).

In this paper we also explore a version of the RSL algorithm that aims to maximise the structural diversity of the states in its selected sample. Width-based planning is one method that has been particularly effective in increasing the structural diversity of states considered during search (Lipovetzky and Geffner 2012; Lipovetzky, Ramírez, and Geffner 2015; Frances et al. 2017; Katz et al. 2017). Width-based planning prunes states considered as non-novel by a defined measure. The original width-based measure introduced by Lipovetzky et al. (2012) is that the novelty of a state is evaluated by the smallest tuple of atoms $t \subseteq s$, where s is the first state that makes t true in the search. Inspired by the success of the width-based novelty algorithms in classical planning, both in progression and regression (Lei and Lipovetzky 2021), we create and experiment with a new novelty based regression algorithm.

Regression Based Supervised Learning

Given a planning problem $\Pi = \langle F, O, I, G \rangle$, RSL produces a training set $\mathcal{D} = \{(s_1, h_1), \dots, (s_N, h_N)\}$ which is a set

of states $s \in S$ paired with goal distance estimates h . To produce \mathcal{D} RSL performs N_r rollouts, each starting at the goal G and applying L times the classical planning regression operator. Each rollout from G is a sequence of actions $\pi^j = (a_i^j)_{i=0}^{L-1}$, for $j = 1, \dots, N_r$. Each π^j produces a sequence of pre-images $x_0^j, x_1^j, \dots, x_L^j$, where $x_0^j = G$ and $x_i^j \subseteq F$. The sequence of pre-images denotes a sequence of sets of states $\mathcal{R}^j = X_0^j, X_1^j, \dots, X_L^j$, where $X_i^j = \{s \mid x_i^j \subseteq s, s \in S\}$. See Figure 1 for an example of this mapping of a pre-image represented by a partial truth assignment into its corresponding set of fully assigned states. By the definition of the regression operator, X_{i-1}^j corresponds with the *pre-image*, conditioned on a_{i-1}^j , of X_i^j . Therefore any state within X_i^j can be reached from X_{i-1}^j by applying action a_{i-1}^j . It follows that any state within X_i^j can reach X_0^j in at most i transitions. Using this observation, RSL labels each state s within its training set of states, T_s , with

$$d(s) = \min(i \mid s \in X_i^j, j \in \{1, \dots, N_r\}) \quad (3)$$

that is, the smallest goal distance estimate of any of the state sets visited by the regressions which s is also a member of.

Algorithm 1: Overview of the RSL Algorithm

Input: Π

Parameter: P_r, L, N_r, N_t, μ

Output: h^{RSL}

- 1: $\mathcal{R} \leftarrow \text{REGRESSION}(\Pi, L, N_r, \mu)$
 - 2: $T_s \leftarrow \text{SAMPLE_STATES}(\mathcal{R}, P_r, N_t)$
 - 3: $\mathcal{D} \leftarrow \text{LABEL}(\mathcal{R}, T_s)$
 - 4: $h^{\text{RSL}} \leftarrow \text{SUPERVISED_LEARNING}(\mathcal{D})$
-

Algorithm 1, provides an overview of RSL. The hyperparameters of RSL are the length of each regression L , the number of regressions to perform N_r , the number of training states to use N_t , the percentage of training states that are randomly sampled from the entire state space P_r , and a function that maps state regression trajectories into novelty levels μ . RSL has three distinct steps, 1: extracting sets of state sets, $\mathcal{R} = \bigcup_{j=1}^{N_r} \mathcal{R}^j$, through performing regressions from the goal set (Alg. 1 line 1), 2: sampling training states T_s and labeling them with goal distance estimates using (3) (Alg. 1 lines 2-3), and 3: training the NN defined heuristic function (Alg. 1 line 4) using empirical risk minimisation (2).

Extracting state sets through regression

As previously explained RSL performs N_r regressions to extract the set of state sets \mathcal{R} over which the training set \mathcal{D} is defined. At step i of a rollout with a pre-image x_i^j corresponding to the set of states X_i^j , as previously defined, the actions we consider valid for pre-imaging X_i^j with are $a \in \nu(x_i^j)$, defined as follows

$$\begin{aligned} \nu(x_i^j) &= \{a \mid a \in \text{REACHABLE}(O, I), \\ &x_i^j \cap \text{e-Del}(a) = \emptyset, \\ &x_i^j \cap \text{Del}(a) = \emptyset, x_i^j \cap \text{Add}(a) \neq \emptyset\} \end{aligned} \quad (4)$$

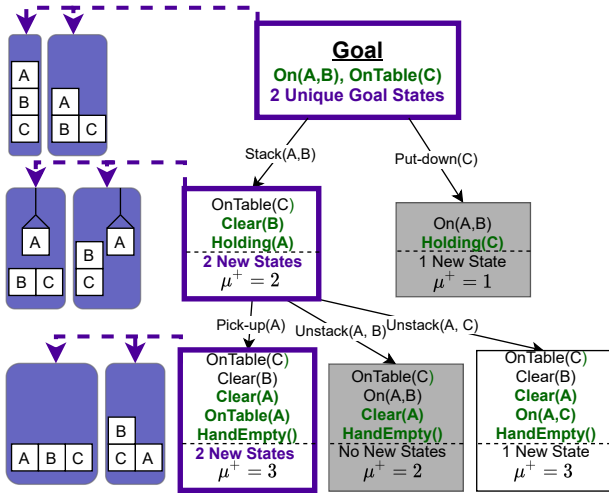


Figure 1: An example rollout performed by N-RSL with $L = 2$ on a 3 block Blocksworld problem. Each square represents a per-image through a partially assigned state with its assigned atoms written within the square. The purple squares represent the example rollout trajectory selected by N-RSL and the possible Blocksworld states for each pre-image along the trajectory are shown on the left. Green atoms are atoms assigned for the first time in the trajectory, and the μ^+ value is calculated using Equation 7.

and $e\text{-Del}(a)$ is

$$e\text{-Del}(a) = \{ q \mid q \in F \setminus \text{Add}(a), \exists p \in \text{Pre}(a) : \text{MUTEX}(p, q) \}. \quad (5)$$

$\text{REACHABLE}(O, I)$ maps the operator set O and initial state I to the set of actions with reachable preconditions in the delete relaxation of Π (Bonet and Geffner 2001) given the initial state of the progression state-transition model I . The $\text{MUTEX}(p, q)$ function in (5) maps the pair of atoms (p, q) to true if p and q are mutually exclusive, that is, it is impossible for p and q to both be true in any state $s \in S$ that can be reached from I . Note that the Ferber et al. (2021) algorithms that use regression also filter the valid actions in the same way through using the mutex groups and applicable operations found by the Fast Downward (FD) (Helmert 2006) Translator¹.

The baseline option for performing the rollout, and the method used by Ferber et al. (2021), is to randomly select actions a for which applying the regression operator is valid. In addition to testing RSL using random action selection we instantiate a version of RSL we name Novelty guided Regression based Learning (N-RSL) that aims to increase the structural diversity of operators selected in its regression.

Preferring actions with novel preconditions For N-RSL at step i of a rollout with a pre-image x_i^j , and a state trajec-

¹See the IS_VALID_WALK parameter in line 848 in code/src/search/task_utils/sampling_technique.cc in Ferber et al.'s (2021) Supplementary Material available at <https://zenodo.org/record/5345958>

tory of $\tau = G, x_1^j, \dots, x_i^j$, N-RSL uses the novelty function μ to select the action a_i to pre-image X_i^j .

$$a_i = \text{argmax}_a \{ \mu(a, \tau) \mid a \in \nu(x_i^j) \} \quad (6)$$

where ties are broken randomly and $\nu(x_i^j)$ is a set of valid actions as described above. Note that for the plain RSL algorithm, which uses random action selection, $\mu = \mu(a, \tau) = 0$ for any $a \in O$ and any state trajectory τ .

In order to increase the structural diversity of the states in sets X_i^j in \mathcal{R}^j we consider how the pre-images x_i^j evolve as we repeatedly apply the regression operator. At each step i of the regression we have a set of valid operators $\nu(x_i^j)$ and a state set X_i^j derived from the pre-image $x_i^j \subseteq F$, where $x_0^j = G$. We propose increasing the structural diversity of the sets extracted by counting the number of atoms an action will assign as true in a pre-image for the first time in the current trajectory. In order to apply this criterion, μ in (6) is replaced by μ^+ below,

$$\mu^+(a, \tau) = |\text{Pre}(a) \setminus \bigcup_{x_i^j \in \tau} x_i^j| \quad (7)$$

This μ^+ measure means N-RSL prefers actions with pre-conditions which contain atoms that are not specified in the goal G and are not a member of the pre-condition set of any of the actions executed in the trajectory up until that point. Note that μ^+ relies only on the current trajectory and is independent of any previously executed regression trajectories. Figure 1 shows an example of a rollout performed on a simple Blocksworld problem with the one-step lookahead method described by (6) using the measure μ^+ defined in (7).

Sampling and Labeling Training Data

The training data for RSL is sampled from the sets of states \mathcal{R} . States are sampled from each set $X_i^j \in \mathcal{R}$, and sampled states that contain mutex atom pairs (p, q) are modified by removing either the p or q atom from the state. Note that if a sampled state from the set X_i^j has a mutex pair (p, q) and $p \in x_i^j$, q will be removed from the state, that is, an atom that is a member of the partial state x_i^j that a state is sampled from will never be removed from the state. As previously described, the labelled heuristic value for a sampled state is given by $d(s)$, which returns the distance of the closest state set in \mathcal{R} to the goal according to the regression.

As we report later, some domains benefited from adding randomly sampled states from S . The random states have mutexes enforced using the same method as above, and are also labeled with $d(s)$. In the case that the state is not a member of any of the sets of states in \mathcal{R} , we define $d(s)$ to equal $L + 1$.

Theorem 1. *Given a problem $\Pi = \langle F, O, I, G \rangle$, N-RSL obtains a training set \mathcal{D} in $\mathcal{O}(|F|(|O|N_rL + N_tLN_r))$ time and $\mathcal{O}(|F|(N_rL + N_t))$ space.*

Proof sketch. RSL performs N_r rollouts and by definition the number of state transitions in each π^j is L . For each

state transition the one step lookahead (Equation 6) considers a maximum of $|O|$ actions and $|O|$ pre-images. Therefore the total number of pre-images considered by RSL is $L \times |O| \times N_r$. Note that both L and N_r are set as constant hyper-parameters and for each pre-image a maximum of $|F|$ atoms need to be considered by the novelty definition μ^+ , therefore the REGRESSION algorithm has a time complexity of $\mathcal{O}(|F||O|N_rL)$. Also for each pre-image a maximum of $|F|$ atoms need to be assigned, hence REGRESSION runs in $\mathcal{O}(|F|N_rL)$ space. Sampling states requires the assignment of at most $|F| \times N_t$ atoms and checking a state’s membership requires at most $|F| \times N_t \times L \times N_r$ comparisons meaning both the SAMPLE_STATES and LABEL algorithms run in $\mathcal{O}(|F||O|N_rL)$ time and $\mathcal{O}(|F|N_t)$ space. \square

Given the training set, \mathcal{D} , any suitable off-the-shelf SL algorithm can be used to obtain a heuristic estimator through optimising the SL objective function (2). We discuss the specifics of one such algorithm in our Experimental Study.

Experimental Study

The experimental study of RSL has two objectives: (1) evaluate the effect of the different mechanisms within the RSL algorithm, and (2) provide a direct comparison to existing NN and model-based heuristic functions.

Methodology

Our benchmark set of domains, instances and initial states is the same as Ferber et al. (2021). As we are learning per instance heuristics, a unique heuristic is trained for each problem instance and then evaluated over a set of 50 different initial states. The 50 initial states were produced by Ferber et al. (2020; 2021), through performing 50 200-step random-walks from the original initial state of the instance. The benchmark instances have also been separated by Ferber et al. (2020; 2021) into “Moderate Tasks”, which are solved by GBFS guided by h^{FF} in less than 900 seconds but more than 1 second, and “Hard Tasks” which are not solved within 900 seconds.

We evaluate h^{RSL} heuristic using the same method as Ferber et al. (2021). Each heuristic is evaluated over 50 different initial states guiding GBFS implemented in FD (Helmert 2006). It is known that a lack of accuracy in heuristics can lead to blow ups in the size of search trees (Helmert, Röger et al. 2008), therefore we can test the relative accuracy of the heuristics by using them in the GBFS and comparing their coverage. The coverage of a planner is defined as the percent of initial states for which a solution path is found within the given planning budget. Ferber et al. (2021) report observing that in general the coverage superiority between the different NN heuristics tested did not vary over time. That is, the planning time used and the relative coverage superiority between the algorithms were not correlated. Given this observation and constraints on our available compute resources we reduce the overall 10 hour planning time-limit that Ferber et al. used by 99% down to just 6 minutes, and compare with the NN defined heuristic baseline algorithms results as provided by Ferber et al. (2021) which use the 10 hour planning time-limit.

As our results are run on different hardware and Ferber et al.’s algorithms use the Keras (Chollet et al. 2015) and the TensorFlow (Abadi et al. 2015) libraries to train and evaluate their NN while we use PyTorch (Paszke et al. 2019), we performed a comparison of the evaluations per second used for commonly solved instances between Ferber et al.’s (2021) methods and $h^{\text{N-RSL}}$. Ferber et al.’s algorithms use the same NN architecture meaning that for the same instance, and assuming the relationship between evaluations and planning time is linear, the evaluations per second should be similar. The data logs provided by Ferber et al. only provide the number of evaluations completed by FD if the problem is solved, therefore we can only compare the ratios of commonly solved instances. Depending on the domain the ratios averaged between 0.3 to 16.1, meaning h^{RSL} ’s evaluations per second were sometimes less but could also be up to 16.1 times higher. A full table of the minimum, maximum and average ratios found for each domain and algorithm can be found in the Supplementary Material. We also benchmark on our hardware an implementation of the SING (Yu, Kuroiwa, and Fukunaga 2020) algorithm which Ferber et al. (2021) did not test and has not previously been applied to this benchmark set. Details of our implementation of the SING algorithm are provided in the Supplementary Material. Finally, we ran the baselines that do not require offline training, h^{FF} and LAMA, on our hardware with the 6 minute time budget.

We define each h^{RSL} heuristic through the same NN architecture used by Ferber et al. (2021). The NN is a *residual network* (He et al. 2016) made up of two dense 250 neuron layers followed by a single residual block with two dense 250 neuron layers followed by a single neuron output. Each neuron in the NN uses the rectified linear activation function. The inputs of the NN are full states of $S(\Pi)$ represented by a Boolean vector $\{0, 1\}^{|F|}$. As Ferber et al. do, we set the *loss* function of the SL optimization problem (2) to be the *mean squared error* (MSE). We use the Adam (Kingma and Ba 2015) stochastic optimization algorithm to find locally optimal solutions of (2), using the following hyper-parameters: learning rate is 10^{-4} , batch size is 64, and maximum number of epochs is set to 1,000. Additionally, we use the *early stopping* heuristic (Duvenaud, Maclaurin, and Adams 2016) setting the *patience* parameter to 2. We split each instance data set into training and validations sets, taking the former 80% and the latter 20% of available samples.

Due to computational constraints we do not tune the architecture or any training parameters of the NN. Note that Ferber et al.’s TSL method trains 10 heuristics functions and selects the best performing heuristic on a set of validation states. We follow this method by running RSL 10 times with different random seeds on each instance to produce 10 heuristic functions. We then test each heuristic over a set of validation states, which are collected using the same method as Ferber et al. (2021), to select the best performing heuristic for each instance. We report both the average coverage of the 10 heuristics learnt and the best heuristic found via the validation method.

Training is run simultaneously for 80 instances over 40 Intel@Xeon@Gold 6138 CPU @ 2.00GHz processor cores

Planning Budget	Ave. over Trials		Methods using Validation							6 minutes h^{FF} LAMA	
	6 minutes h^{RSL}	h^{N-RSL}	6 minutes h^{RSL}	h^{N-RSL}	h^{Boot}	h^{BExp}	600 minutes* h^{AVI}	h^{TSL}	h^{HGN}		
Moderate Tasks											
blocks	80.0	91.5	99.2	100	18.0	0.0	0.0	80.4	100	100	100
depot	48.7	58.8	77.0	89.0	60.3	32.7	54.7	90.3	0.0	93.7	99.3
grid	71.0	60.3	100	97.0	100	100	51.0	93.0	0.0	90.0	100
npuzzle	15.3	18.9	25.2	46.8	28.0	0.0	1.0	0.0	0.3	92.8	97.8
pipeworld	70.7	69.6	85.8	82.6	57.8	68.4	50.2	92.2	7.6	63.0	98.6
rovers	12.6	12.5	15.0	15.8	48.2	21.8	45.0	26.0	14.0	79.5	100
scanalyzer	87.4	94.1	100	100	33.3	70.7	67.3	82.7	11.0	91.7	100
storage	16.1	16.4	17.0	18.0	89.0	57.5	69.5	24.5	0.0	27.5	34.0
transport	74.8	70.8	100	93.8	100	100	87.5	99.2	94.7	100	100
visitall	93.6	95.4	99.7	98.0	55.3	0.0	0.0	0.0	100	89.0	100
Average	57.0	58.8	71.9	74.1	59.0	45.1	42.6	58.8	32.8	82.7	93.0
Average Train Time/Inst. (Hr)	0.37	0.38	3.68	3.75	112*				13.1*	-	
Hard Tasks											
blocks	18.5	45.3	36.4	68.0	0.0	0.0	0.0	0.0	50.0	46.4	96.0
depot	4.0	3.3	14.6	12.6	8.3	4.3	12.9	35.4	0.0	9.4	69.4
grid	21.9	32.1	67.2	69.0	87.8	95.0	70.5	60.2	0.0	31.0	100
npuzzle	0.0	0.0	0.0	0.0	0.0	0.0	0.0	0.0	0.0	5.8	12.8
pipeworld	27.4	25.0	33.8	33.1	23.4	19.1	8.0	48.7	0.0	20.4	68.0
rovers	0.0	0.1	0.1	0.1	2.8	0.8	6.5	1.5	0.3	8.3	100
scanalyzer	86.4	89.7	100	100	3.3	0.0	60.7	60.0	0.0	83.3	100
storage	3.7	2.5	1.8	0.2	27.2	13.2	15.8	0.0	0.0	9.2	9.0
transport	0.0	1.2	0.0	8.8	0.0	0.0	2.4	0.0	0.0	0.0	59.6
visitall	82.4	91.8	100	100	28.0	0.0	0.0	0.0	100	40.0	100
Average	24.4	29.1	35.4	39.2	18.1	13.3	17.7	20.6	15.0	25.4	71.5
Average Train Time/Inst. (Hr)	0.69	0.69	6.88	6.88	112*				10.4*	-	

Table 1: Comparison of the coverage of h^{RSL} with other Neural Network defined heuristics functions introduced by Ferber et al. (2021) h^{Boot} , h^{BExp} , h^{AVI} , as well as the h^{TSL} introduced by Ferber et al. (2020), and h^{HGN} from Shen et al. (2020). The table also shows the coverage of h^{FF} (Hoffmann and Nebel 2001) and LAMA (Richter and Westphal 2010) (run on same hardware as RSL). Note that h^{HGN} trains one heuristic per domain not instance with training budgets between 14.7 and 112 CPU hours. The bold numbers indicate the highest coverage among the Neural Network methods. *Note that the baseline learning methods that use a 600 minute planning budget are the values as reported by Ferber et al. (2021). According to standard single thread CPU benchmarks, our vCPU can be 20% faster. We provide a discussion of the impact of discrepancies in hardware and software in the Methodology Section.

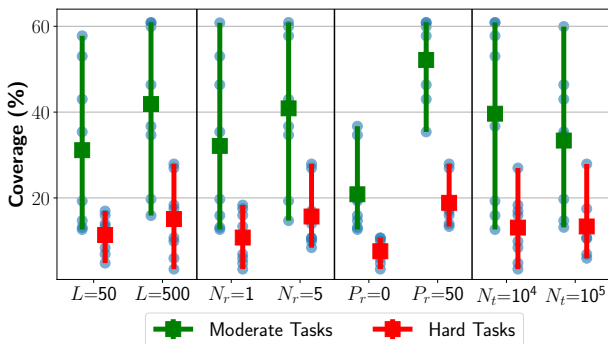
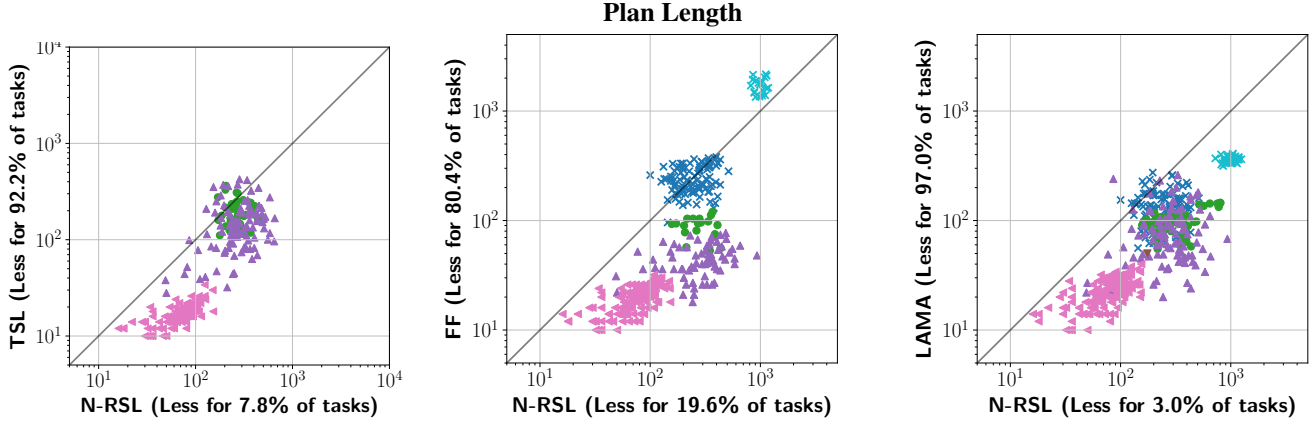
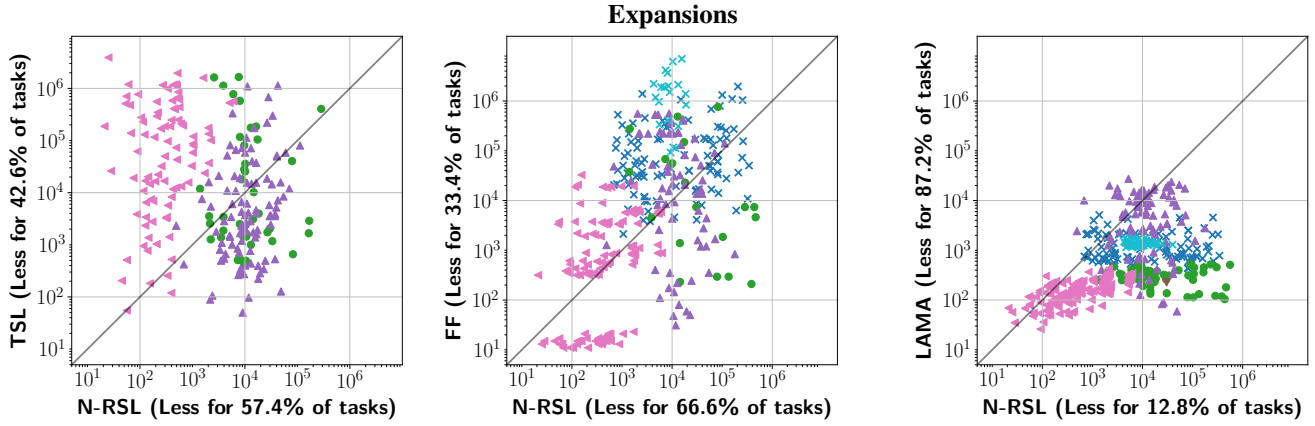


Figure 2: A summary of the average coverage over the “Moderate” and “Hard” tasks for 16 different configurations of RSL. The 4 boxes each show a different segmentation of the 16 configurations according to the value of a single hyper-parameter. Each configuration’s coverage is marked with a blue dot and the lines show the range of coverage over the configurations with the mean marked with a square.

with 720GB of shared RAM, limiting each training instance to run on a single vCPU (each CPU core has 2 vCPUs). For training the h^{RSL} heuristic, the Tarski framework (Francés and Ramírez 2021) is used to ground each problem instance in order to get the F , O , and G sets used for the regressions. In line with the h^{Boot} , h^{BExp} , h^{AVI} and h^{SL} heuristics, the FD translator is used for identifying a set of state mutexes to enforce, for both the state sampling and valid actions for the regression operator as described in the previous Section. For evaluation we use the same hardware, along with Downward lab (Seipp et al. 2017) to run 80 FD searches at once limiting each FD search to run on a single vCPU with a maximum of 3.8 GB of memory. The PyTorch library (Paszke et al. 2019) is used for the training and evaluations of RSL’s NN. The RSL code, result files and additional implementation details are included in the Supplementary Material.

Results

First we present the results from a grid search over the hyper-parameters of RSL. To maximise the number of hyper-



× blocks + depot ● grid ■ npuzzle ▲ pipesworld ▼ rovers ◀ scanalyzer ▶ storage ◆ transport × vitalis

Figure 3: Pairwise comparisons over commonly solved tasks between h^{N-RSL} using the validation method, and the best performing baseline NN based heuristic function h^{TSL} and model-based methods h^{FF} and LAMA over the “Hard Tasks” benchmark set. The top row shows the scatter plot of the number of expansions used by each search algorithm while the bottom row shows the plan length found by each algorithm. The percentage value, shown in the axis titles, is the percentage of the commonly solved tasks that the relevant algorithm required fewer expansions or discovered a shorter plan than the algorithm it is being compared to. Note that tasks which are not solved by at least one of the algorithms in the pair are not included in these graphs. Graphs were generated using Downward Lab (Seipp et al. 2017).

parameter combinations we could test with our limited computational resources, we evaluated each trained heuristic from the grid search on 10 out of the 50 initial states for each of the 143 instances in the benchmark set. Figure 2 summarises the impact of each of the hyper-parameter values tested on the average coverage of h^{RSL} across the benchmark set. For the hyper-parameter grid search we tested 16 different settings over the different combinations of $N_t = 10,000$ or 100,000, $P_r = 0$ or 50, $N_r = 1$ or 5, and $L = 50$ or 500. The Supplementary Material includes a table detailing the different configurations tested along with their average coverage over each domain. Figure 2 shows that the value of P_r has the biggest influence on the average coverage over the benchmark set of h^{RSL} used in GBFS. This observation shows the importance of including states in the training set that are not within any of the sets of states visited by the rollouts from the goal set. Figure 2 also suggests that RSL benefits from using more than one rollout for extracting training states and considering 500 applications of the regression operator instead of 50. Interestingly, Figure 2 shows that train-

ing with 10,000 or 100,000 states does not influence the performance in an obvious way. However, overall the best performing set of hyper-parameters over the “Hard Tasks” which we use for all experiments from this point forth are $N_t = 100,000$, $P_r = 50$, $N_r = 5$, and $L = 500$.

Table 1 shows a comparison of existing methods with respect to RSL and N-RSL, using the best performing configuration from the hyper-parameter grid search. The SING algorithm is omitted from Table 1 due to poor performance but its results are included in the Supplementary Material. The first notable difference is the average training times used by each algorithm. h^{RSL} without validation uses less than 1% of the training CPU time used by all the other per-instance NN defined heuristic functions for both the “Moderate” and “Hard” task sets. Even when using the validation method which requires 10 RSL executions the training time used is less than 7% of the per-instance NN methods. The overall average coverage over the benchmark set shows that h^{RSL} and h^{N-RSL} outperform the other NN defined heuristic functions for the “Hard Tasks” with and without using the

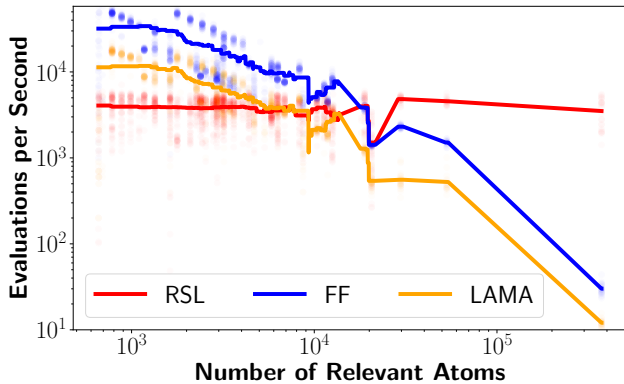


Figure 4: The number of heuristic evaluations per second versus the number of relevant atoms as determined by FD translator’s reachability analysis for a set of commonly solved problem instances between h^{RSL} , h^{FF} and LAMA. Each dot represents the values for a single problem instance and the line represents the moving average with a window size of 2000 atoms.

validation method. h^{RSL} and $h^{\text{N-RSL}}$ when using the validation method also outperform the other NN heuristics on the “Moderate Tasks”. The model-based method LAMA clearly dominates all other methods. The model-based heuristic h^{FF} also outperforms h^{RSL} and $h^{\text{N-RSL}}$ on the “Moderate Tasks”, however on the “Hard Tasks” h^{RSL} with validation and $h^{\text{N-RSL}}$ with and without validation have better overall performance. While $h^{\text{N-RSL}}$ has better average coverage than h^{RSL} the difference is small with a 1.8% and 4.7% average improvement over the “Moderate” and “Hard Tasks” respectively when no validation is used.

Figure 3 provides additional insights into the performance of $h^{\text{N-RSL}}$ compared to the best performing baseline algorithms. For commonly solved tasks, h^{TSL} on average produces higher quality plans than $h^{\text{N-RSL}}$. This observation could be a result of h^{TSL} having higher quality labels used in training. h^{TSL} uses h^{FF} with GBFS to label sampled states in the train set, while $h^{\text{N-RSL}}$ labels states with goal distance estimates derived from the state sets visited by N-RSL’s regressions. The objective of h^{FF} with GBFS is to find the shortest path from a state to the goal state, while the objective of N-RSL’s regression is to maximise a defined novelty measure (Equation 6) with the aim of finding the shortest path that visits the most number of reachable atoms $a \in F$. This trade-off between exploration and exploitation shows through in the results where $h^{\text{N-RSL}}$ has a higher coverage than h^{TSL} over a diverse set of initial states but produces lower quality plans in terms of plan length among the commonly solved tasks. This behaviour is also displayed when comparing directly to the h^{FF} heuristic, while LAMA dominates $h^{\text{N-RSL}}$ in both coverage and plan quality.

Figure 4 shows that for smaller problem instances the model-based methods h^{FF} , and LAMA are able to compute a higher number of evaluations per second than h^{RSL} . However, h^{RSL} ’s evaluations per second stays relatively constant

while the model-based methods evaluations per second decreases as problem instances become larger.

Discussion

The heuristic values from the NN defined heuristic functions we report in this paper are calculated by taking the linear combination of the outputs of the last hidden layer of the NN. We note that the NN heuristics discussed in this paper and those of Ferber et al. (2020; 2021) are an application of *state aggregation* (Bertsekas 2018), a well-known technique in Approximate Dynamic Programming. For each of the different problem instances we explored in this paper, the size of the last hidden layer was fixed at 250 neurons. It is possible that for harder problem instances a feature vector larger than 250 is required in order to produce more useful heuristics. Ferber et al. (2020) have performed an investigation into effects of the NN architecture in terms of the activation functions used and the number of hidden layers, however they did not explore the number of neurons used within the hidden layers. One avenue of future work is to investigate the impact of scaling the number of neurons used within the hidden layers of the NN so the capacity (Goodfellow, Bengio, and Courville 2016) of the NN scales too with the size of the planning instance.

However, one advantage we observed of the NN heuristic functions over the model-based heuristics in Figure 4 is that the gap in number of evaluated states per second narrows until it eventually disappears, so the NN heuristic becomes significantly faster in comparison (and less informed too, probably) as the problem size increases. This is because only the input layer size changes according to $|F|$ for the NN architecture used in this work, while the rest of the neurons and edges remain constant. That is, as the input layer has $|F|$ neurons and the first hidden layer has 250 neurons there are $|F| \times 250$ edges joining the two layers resulting in the NN evaluations being in $O(|F|)$ time. Conversely, h^{FF} requires completing a search over the problem with the delete relaxation which has time-complexity that is polynomial over the number of actions and reachable atoms (Hoffmann and Nebel 2001).

Future work should investigate NN heuristics like h^{RSL} over problems that are too large for h^{FF} or LAMA to produce enough evaluations per second to be useful. It is possible that a NN defined heuristic function will be able to produce a large enough number of evaluations per second to be useful over these large domains, even if the heuristic is less informed than the model-based heuristics. Last, we have shown that h^{RSL} and $h^{\text{N-RSL}}$ have good performance while requiring significantly smaller resources than the NN-based baselines considered in the paper. We think that this encouraging result supports the assumption that RSL and follow-up methods can be used to obtain useful heuristic functions for large instances of challenging combinatorial optimization problems.

References

- Abadi, M.; Agarwal, A.; Barham, P.; Brevdo, E.; Chen, Z.; Citro, C.; Corrado, G. S.; Davis, A.; Dean, J.; Devin, M.; Ghemawat, S.; Goodfellow, I.; Harp, A.; Irving, G.; Isard, M.; Jia, Y.; Jozefowicz, R.; Kaiser, L.; Kudlur, M.; Levenberg, J.; Mané, D.; Monga, R.; Moore, S.; Murray, D.; Olah, C.; Schuster, M.; Shlens, J.; Steiner, B.; Sutskever, I.; Talwar, K.; Tucker, P.; Vanhoucke, V.; Vasudevan, V.; Viégas, F.; Vinyals, O.; Warden, P.; Wattenberg, M.; Wicke, M.; Yu, Y.; and Zheng, X. 2015. TensorFlow: Large-Scale Machine Learning on Heterogeneous Systems. Software available from tensorflow.org.
- Arfaee, S. J.; Zilles, S.; and Holte, R. C. 2011. Learning heuristic functions for large state spaces. *Artificial Intelligence*, 175(16-17): 2075–2098.
- Bellman, R. 1957. *Dynamic Programming*. Princeton University Press.
- Bertsekas, D. P. 2018. Feature-based aggregation and deep reinforcement learning: A survey and some new implementations. *IEEE/CAA Journal of Automatica Sinica*, 6(1): 1–31.
- Bonet, B.; and Geffner, H. 2001. Planning as heuristic search. *Artificial Intelligence*, 129(1): 5–33.
- Bonet, B.; Loerincs, G.; and Geffner, H. 1997. A robust and fast action selection mechanism for planning. In *AAAI/IAAI*, 714–719.
- Chollet, F.; et al. 2015. Keras. <https://keras.io>.
- Duvenaud, D.; Maclaurin, D.; and Adams, R. 2016. Early stopping as nonparametric variational inference. In *Artificial Intelligence and Statistics (AISTATS)*, 1070–1077.
- Edelkamp, S. 2014. Planning with pattern databases. In *Sixth European Conference on Planning*, 84–90.
- Ferber, P.; Geiber, F.; Trevizan, F.; Helmert, M.; and Hoffmann, J. 2021. Neural Network Heuristic Functions for Classical Planning: Reinforcement Learning and Comparison to Other Methods. In *2nd PRL Workshop, International Conference on Automated Planning and Scheduling*.
- Ferber, P.; Helmert, M.; and Hoffmann, J. 2020. Neural network heuristics for classical planning: A study of hyperparameter space. In *European Conference on Artificial Intelligence*, 2346–2353.
- Fikes, R. E.; and Nilsson, N. J. 1971. STRIPS: A new approach to the application of theorem proving to problem solving. *Artificial intelligence*, 2(3-4): 189–208.
- Francés, G.; and Ramírez, M. 2021. Tarski - An AI Planning Modeling Framework. <https://github.com/aig-upf/tarski>.
- Francés, G.; Ramírez, M.; Lipovetzky, N.; and Geffner, H. 2017. Purely declarative action descriptions are overrated: Classical planning with simulators. In *International Joint Conference on Artificial Intelligence*, 4294–4301.
- Geffner, H.; and Bonet, B. 2013. A concise introduction to models and methods for automated planning. *Synthesis Lectures on Artificial Intelligence and Machine Learning*, 8(1): 1–141.
- Goodfellow, I.; Bengio, Y.; and Courville, A. 2016. *Deep learning*. MIT press.
- Hardt, M.; and Recht, B. 2021. *Patterns, predictions, and actions: A story about machine learning*. <https://mlstory.org>.
- He, K.; Zhang, X.; Ren, S.; and Sun, J. 2016. Deep residual learning for image recognition. In *IEEE Conference on Computer Vision and Pattern Recognition*, 770–778.
- Helmert, M. 2006. The fast downward planning system. *Journal of Artificial Intelligence Research*, 26: 191–246.
- Helmert, M.; Haslum, P.; Hoffmann, J.; et al. 2007. Flexible Abstraction Heuristics for Optimal Sequential Planning. In *International Conference on Automated Planning and Scheduling*, 176–183.
- Helmert, M.; Röger, G.; et al. 2008. How Good is Almost Perfect?. In *AAAI*, volume 8, 944–949.
- Hoffmann, J.; and Nebel, B. 2001. The FF planning system: Fast plan generation through heuristic search. *Journal of Artificial Intelligence Research*, 14: 253–302.
- Katz, M.; Lipovetzky, N.; Moshkovich, D.; and Tuisov, A. 2017. Adapting novelty to classical planning as heuristic search. In *International Conference on Automated Planning and Scheduling*, 172–180.
- Kingma, D. P.; and Ba, J. 2015. Adam: A method for stochastic optimization. In *International Conference on Learning Representations*.
- Lei, C.; and Lipovetzky, N. 2021. Width-Based Backward Search. In *International Conference on Automated Planning and Scheduling*, 219–224.
- Lipovetzky, N.; and Geffner, H. 2012. Width and Serializa-tion of Classical Planning Problems. In *European Conference on Artificial Intelligence*, 540–545.
- Lipovetzky, N.; Ramírez, M.; and Geffner, H. 2015. Classical planning with simulators: results on the Atari video games. In *International Joint Conference on Artificial Intelligence*, 1610–1616.
- Paszke, A.; Gross, S.; Massa, F.; Lerer, A.; Bradbury, J.; Chanan, G.; Killeen, T.; Lin, Z.; Gimelshein, N.; Antiga, L.; Desmaison, A.; Kopf, A.; Yang, E.; DeVito, Z.; Raison, M.; Tejani, A.; Chilamkurthy, S.; Steiner, B.; Fang, L.; Bai, J.; and Chintala, S. 2019. PyTorch: An Imperative Style, High-Performance Deep Learning Library. In *Advances in Neural Information Processing Systems 32*, 8024–8035.
- Richter, S.; and Westphal, M. 2010. The LAMA planner: Guiding cost-based anytime planning with landmarks. *Journal of Artificial Intelligence Research*, 39: 127–177.
- Rintanen, J. 2008. Regression for classical and nondeterministic planning. In *European Conference on Artificial Intelligence*, 568–572.
- Seipp, J.; Pommerening, F.; Sievers, S.; and Helmert, M. 2017. Downward Lab. <https://doi.org/10.5281/zenodo.790461>.
- Shen, W.; Trevizan, F.; and Thiébaux, S. 2020. Learning domain-independent planning heuristics with hypergraph networks. In *International Conference on Automated Planning and Scheduling*, 574–584.
- Yu, L.; Kuroiwa, R.; and Fukunaga, A. 2020. Learning Search-Space Specific Heuristics Using Neural Network. *12th HSDIP Workshop, International Conference on Automated Planning and Scheduling*, 1–8.

Supplementary Material

Additional RSL Implementation Details

For the NN training we use the Adam optimizer (Kingma and Ba 2015) with a learning rate of 10^{-4} , initial decay rates of $\beta^1 = 0.9$ and $\beta^2 = 0.999$, and $\epsilon = 10^{-8}$. Additionally we use a batch size of 64, a maximum of 1,000 training epochs, and early stopping with a patience of 2, using a split of training samples of 80-20 for training and validation, respectively.

Comparison of Evaluations per Second of Baseline Results

Table 3 shows the evaluations per second ratios between our h^{RSL} FastDownward runs and the baseline algorithms run by Ferber et al. (2021).

SING Implementation Details

We implemented the configuration C4 of the SING algorithm (Yu, Kuroiwa, and Fukunaga 2020) as described by Yu et al. but using the same NN architecture, loss function and training hyper-parameters as used for RSL. 10^5 samples were used for training, which were collected using a budget of 500 samples per DFS resulting in 200 total DFS rollouts.

Additional Results

The results for our implementation of SING are shown in Table 2. The performance of SING is very poor compared to the results of the other baselines shown in Table 1 in the main paper. We also performed individual runs of instances using SING with the same NN architecture, loss function, number of training samples, and number of samples per DFS as described by Yu et al. (2020), however the performance observed was still poor. Yu et al. mention that they perform manual tuning of hyper-parameters but do not provide the selected parameters used by the NN training algorithm, which could be the reason for the poor performance observed in our results.

Table 4 shows the results of each configuration tested in the RSL hyper-parameter grid search.

	Moderate Tasks	Hard Tasks
blocks	17.6	0.8
depot	0.0	0.0
grid	0.0	0.0
npuzzle	0.0	0.0
pipesworld	13.8	0.1
rovers	6.2	0.0
scanalyzer	16.7	0.0
storage	0.0	1.0
transport	0.0	0.0
visitall	1.3	0.0
Average	5.6	0.2
Average Train Time/Inst. (Hr)	1.6	2.6

Table 2: Coverage of the heuristic learnt by SING (as detailed in the “SING Implementation Details” Section) in GBFS using a planning time limit of 6 minutes.

	h^{Boot}			h^{BExp}			h^{AVI}			h^{TSL}		
	Ave	Min	Max	Ave	Min	Max	Ave	Min	Max	Ave	Min	Max
blocks	1.2	0.7	5.0	-	-	-	-	-	-	2.3	0.4	6.8
depot	1.2	0.8	1.4	1.2	1.0	1.5	1.2	0.9	2.5	3.9	0.7	9.9
grid	3.1	0.6	43.8	1.3	0.5	12.7	15.8	0.7	79.8	13.2	4.2	80.5
npuzzle	1.1	0.8	2.3	-	-	-	1.5	1.0	2.5	-	-	-
pipesworld	1.4	0.3	8.0	1.4	0.7	10.8	1.4	0.3	19.7	7.8	0.8	82.6
rovers	14.6	0.9	70.1	15.3	0.9	72.3	16.1	0.9	85.6	13.7	0.3	43.4
scanalyzer	1.1	0.1	23.2	0.3	0.03	0.9	1.2	0.1	9.5	8.6	0.2	45.8
storage	1.5	0.8	4.5	1.3	0.8	2.0	1.2	0.8	1.6	3.3	1.0	6.4
transport	1.3	0.8	3.8	1.1	0.9	1.7	1.0	0.7	2.9	5.0	0.6	11.2
visitall	0.9	0.4	1.5	-	-	-	-	-	-	-	-	-

Table 3: Ratios of evaluations per second of our h^{RSL} verse the baseline methods run by Ferber et al. (2021) for commonly solved instances.

N_t	10,000								100,000							
	0				50				0				50			
	1	5	50	500	1	5	50	500	1	5	50	500	1	5	50	500
P_r																
N_r																
L	50	500	50	500	50	500	50	500	50	500	50	500	50	500	50	500
Moderate Tasks																
blocks	0.0	58.4	20.8	99.2	99.2	93.6	92.4	100.0	0.0	60.0	0.0	99.6	94.8	99.6	100.0	98.8
depot	0.0	0.3	20.3	12.3	59.7	61.3	79.3	79.3	2.3	0.0	0.7	1.7	34.3	43.7	69.3	51
grid	0.0	0.0	0.0	1.0	21.0	84.0	50.0	40.0	0.0	0.0	0.0	5.0	16.0	9.0	1.0	48
npuzzle	0.0	0.0	0.0	0.0	0.2	28.8	1.2	28.8	0.0	0.0	0.0	0.0	0.0	17.2	1.2	34.8
pipesworld-nt	11.8	15.8	17.6	23.6	28.6	41.4	27.2	48	21.6	26	31.4	23.4	27	41	30	39
rovers	6.5	6.2	6.5	7.2	11.5	3	12.5	12.8	6.5	6.2	4.5	5.2	7.5	1.8	10	8.5
scanalyzer	100.0	65.3	100.0	87	100.0											
storage	0.0	0.0	12	0.0	24.5	7	24	0.0	1	0.0	7	0.0	8.0	0.0	29	35.5
transport	8.2	0.0	11.5	42.8	98.8	97	99.2	100.0	0.0	0.0	1.8	32.8	49	70.8	62.8	84.8
visitall	0.0	13	4.3	94	86.7	92	92	100.0	0.0	5	1.7	79	17.3	80.7	26.7	99
Average	12.7	15.9	19.3	36.7	53.0	60.8	57.8	60.9	13.1	19.7	14.7	34.7	35.4	46.4	43.0	59.9
Hard Tasks																
blocks	0.0	0.0	0.0	18.4	41.6	44.4	34.4	34.4	0.0	0.0	0.0	12.8	27.6	42	24	41.2
depot	0.0	0.0	0.0	0.0	6	8	13.1	8.3	0.0	0.0	0.0	0.0	0.3	5.4	4.9	10.6
grid	0.0	0.0	0.0	0.0	0.0	8	0.2	0.8	0.0	0.0	0.0	0.0	0.0	0.0	0.0	5.2
npuzzle	0.0	0.0	0.0	0.0	0.0	0.0	0.0	0.0	0.0	0.0	0.0	0.0	0.0	0.0	0.0	0.0
pipesworld-nt	0.1	0.1	0.8	4.5	5.3	8.6	5.5	12.1	2.2	5.4	4.4	8.1	4.8	12.4	8.8	8.8
rovers	0.0	0.0	0.0	0.0	0.0	0.0	0.0	0.1	0.0	0.0	0.0	0.0	0.0	0.0	0.0	0.0
scanalyzer	48	34	83.3	66	100.0	96.7	100.0	100.0	66.7	54	98.7	81.3	100.0	70.7	100.0	100.0
storage	0.0	0.0	0.0	0.0	6.8	8	8.2	0.0	0.0	0.0	2.5	3	0.8	0.2	2	12.5
transport	0.0	0.0	0.0	0.0	0.0	3.6	0.0	14	0.0	0.0	0.0	0.0	0.0	0.0	0.0	0.8
visitall	0.0	0.0	0.0	10	0.0	6	8	100.0	0.0	0.0	0.0	2	0.0	44	0.0	100
Average	4.81	3.41	8.41	9.89	15.97	18.33	16.94	26.97	6.89	5.94	10.56	10.72	13.35	17.47	13.97	27.91

Table 4: Comparison of the coverage given a 6 minute planning time budget of h^{RSL} using a range of different hyper-parameter values. Each run uses only a single trial and is evaluated over 10 of the 50 initial states for each instance in the benchmark set.